Article

Synthesis of a Family of Pd(II) Complexes Using Pyridyl-Ketone Ligands: Crystal Structure, Thermal, Physicochemical, XRD/HSA, Docking, and Heck Reaction Application

Published as part of ACS Omega virtual special issue "3D Structures in Medicinal Chemistry and Chemical Biology".

Anas AlAli, Khalil Shalalin, Abeer AlObaid, Khaled Alkanad, Abdelkader Zarrouk, Ismail Warad,* and Shaukath Ara Khanum*

Cite This: *ACS Omega* 2024, 9, 25073−25083

Read Online

ACCESS | 📊 Metrics & More | 📖 Article Recommendations | 🆘 Supporting Information

ABSTRACT: Four Pd(II) complexes, (dpk)PdCl$_2$ (complex-1), and (dpk)Pd(OAc)$_2$ (complex-2) have been prepared using di(2-pyridyl) ketone as the chelate ligand (dpk). The (dpk·EtOH)PdCl$_2$ (complex-3) and (dpk·EtOH)Pd(OAc)$_2$ (complex-4) were synthesized by selectively introducing complex-1 and complex-2 to an EtOH in situ nucleophilic addition reaction on the O═C of the dpk ligand, respectively. All complexes were characterized using CHN-EA, UV−vis, FT-IR, FAB-MS, EDX, TGA, and NMR physicochemical tools. The XRD-crystallography technique was employed to ascertain the structure of complex-3. The analysis revealed a monoclinic/$P2_1/c$ crystal system characterized by a square planar structure oriented in the *cis* direction around the Pd center. Several C−H···Cl and O−H···O H-bonds constructing 2D-S12 and S7 synthons were confirmed via XRD/HSA interactions. The influence of EtOH addition to the O═C group of dpk in (dpk)PdCl$_2$ was documented by using UV−vis/FT-IR spectra and TGA analysis. As catalysts, all complexes have demonstrated a notable catalytic function in the Heck reaction, resulting in a high yield under gentle conditions using iodobenzene and methyl acrylate as model reactions. Moreover, the complex-1 and complex-3 docking activity was evaluated against 1BNA-DNA.

Heck Catalyst
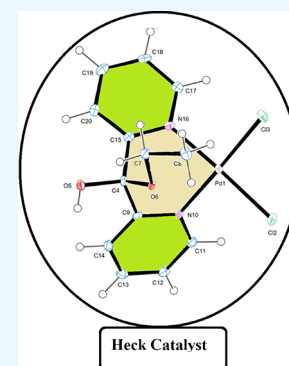
1. INTRODUCTION

The di(2-pyridyl) ketone (dpk) has gained attention as a chelate ligand due to its ability to bond with various coordination modes. It is a commonly utilized ligand for metals, and numerous studies have investigated its interactions with metal ions.[1−4] Mononuclear transition metal complexes of the dpk ligand were isolated when it acts a nitrogen bidentate ligand; mostly polynuclear or cluster transition metal complexes were expected if the carbonyl oxygen atom bonded to the metal center.[4−7] The neutral dpk molecule can act as a bidentate ligand by forming bonds through the N, O or N, N atoms. Alternatively, it can be a tridentate ligand by forming additional bonds through the N, N, and O atoms.[7−12] Moreover, when coordinated to M-centers, the O═C group was subjected to nucleophilic addition reactions, such as the addition of water, revealing the formation of its hydrated gem-diol or alcohol, resulting in alcoholate dpk.ROH formation. Afterward, dpk can undergo an in situ procedure to convert into another ligand type, a transformation that cannot be accomplished by traditional organic methods.[1,3] In this work, the carbonyl of ketone in (dpk)PdX$_2$ complex undergoes alcoholation in the existence of ROH (e.g., ethanol), an "ethanolated" (dpk·EtOH)PdX$_2$ hemiketal complex was formed. The in situ ethanoate reaction of (dpk)PdCl$_2$ to

form (dpk.EtOH)PdCl$_2$ was tracked by UV−vis/IR and proven by single-crystal X-ray single crystal measurement. The utilization of Pd(II)-complexes in the Heck cross-coupling process as a means to catalyze the introduction of aryl groups onto alkenes using organic halides is widely regarded as an exceptionally adaptable and potent method for generating new carbon−carbon bonds.[13−22]

As part of our continued focus on palladium(II) chelate catalyst chemistry for the C−C Heck reaction,[21] we prepare and structurally identify all complexes produced from the dpk ligand in this study. The thermal behaviors of complex-1 and complex-3 before and after alcoholization have been determined. The catalytic investigation of all complexes in Heck processes using iodobenzene and methyl acrylate as the model reaction has also been carried out under easy coupling easy conditions. Moreover, the in silico docking behavior

against 1BNA-DNA for complex-1 and complex-3 has been evaluated.

2. EXPERIMENTAL SECTION

2.1. Materials and Instrumentations. All reactions were conducted under an inert argon atmosphere, employing typical high-vacuum and Schlenk-line techniques. $Pd(OAc)_2$, $PdCl_2(PhCN)_2$, and dpk were obtained from ChemPur and Merck and utilized without further modifications. An elemental analysis was conducted using an Elementar Varrio EL analyzer. The Bruker DRX 250 spectrometer was used to record high-resolution ^1H, $^{13}C\{^1H\}$, and DEPT 135 NMR spectra at a temperature of 298 K. Additionally, FT-IR and FAB-MS data were acquired using a Bruker IFS 48 FT-IR spectrometer and a Finnigan 711A (8 kV) spectrometer, respectively. After being edited by AMD, the FAB-MS data was reported as mass/charge (m/z). The C−C coupling tests were analyzed using a GC 6000 Vega Gas 2 instrument (manufactured by Carlo Erba Instrument) equipped with a Flame Ionization Detector (FID) and a PS 255 capillary column (20 m in length). The carrier gas used was helium at a pressure of 40 kPa. The data was integrated using a 3390 A integrator (manufactured by Hewlett-Packard).

2.2. Synthesis of Complex-1 and Complex-2. A 0.40 mmol portion of Pd(II) salt was dissolved in 30 mL of CH_2Cl_2 and added to 10 mL of dpk (0.41 mmol). The reaction mixture was agitated for 1 h at RT, producing a clear red-colored solution. The solution was condensed to a volume of 1 mL using decreased pressure. The addition of 20 mL of n-hexane resulted in the formation of brown particles, which were then filtered and thoroughly washed with diethyl ether.

Complex-1.
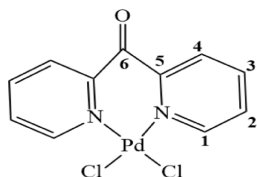
Complex-1

Yield: 82%, ^1H NMR (CDCl_3): δ (ppm): 8.72 (d, 2H, H1, J = 5.21 Hz); 8.07 (d, 2H, H4, J = 7.70 Hz); 7.87 (dd, 2H, H2, J = 7.67 Hz); 7.46 (dd, 2H, H3, J = 5.13 Hz); $^{13}C\{^1H\}$ NMR (CDCl_3): 193.78 (C6); 152.34 (C5); 150.29 (C1); 137.73 (C3); 128.47 (C2); 121.70 (C4). *CHN Anal.* Found: C, 36.17; H, 2.12; N, 7.79%, calculated from $C_{11}H_8Cl_2N_2OPd$ formula C, 36.55; H, 2.23; N, 7.75%. Theor. MS [M]$^+$ 360.1 found [M-1]$^+$ 359.8 m/z. IR, (KBr, cm^{-1}): 3088 (Py−H); 2905−2858 (alkyl-H); 1655 (C=O), 1566 (C=N); 1533−1443 (C=C), 680−500 (Pd−N).

Complex-2.
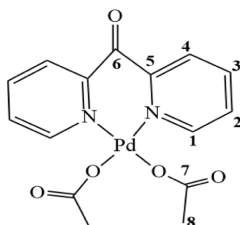
Complex-2

Yield: 76%, ^1H NMR (CDCl_3): δ (ppm): 8.92 (d, 2H, H1, J = 4.41 Hz); 8.32 (d, 2H, H4, J = 7.88 Hz); 8.22−7.85 (m, H2

and H3); 2.25 (s, 6H, H8); $^{13}C\{^1H\}$ NMR (CDCl_3): 185.66 (C6); 180.24 (C7), 153.45 (C5); 149.23 (C1); 137.22 (C3); 123.54 (C2); 120.97 (C4); 21.12 (C8). *CHN Anal.* Found: C, 44.23; H, 3.54; N, 6.65%, calculated from the $C_{15}H_{14}N_2O_5Pd$ formula C, 44.08; H, 3.45; N, 6.85%. Theor. MS [M]$^+$ 408.1 found [M-1]$^+$ 407.2 m/z. IR, (KBr, cm^{-1}): 3104 (Py−H); 2915−2825 (alkyl-H); 1652 (C=O), 1562 (C=N); 1522−1434 (C=C), 680−500 (Pd−N).

2.3. Synthesis of Complex-3 and Complex-4. A solution of 1 or 2 (0.20 mmol) was dissolved in a mixture of dichloromethane/ethanol (1 to 5). The reaction mixture was subjected to ultrasonication for 10 min to ensure complete solubility and then sealed and stirred for 24 h. The solution was concentrated to a 1 mL volume under reduced pressure. The addition of 20 mL diethyl ether caused the precipitation of light red solids, which were filtrated, then washed well with n-hexane, and dried under vacuum.

Complex-3.
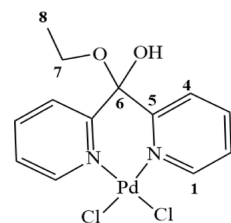
Complex-3

Yield: 71%, ^1H NMR (CDCl_3): δ (ppm): 8.84 (d, 2H, H1, J = 4.88 Hz); 8.24 (d, 2H, H4, J = 7.82 Hz); 8.12−7.90 (m, 4H, H2 and H3); 4.43 (s, 1H, OH); 3.71 (q, 2H, H7, J = 7.04 Hz); 1.21 (t, 3H, H8, J = 7.02 Hz); $^{13}C\{^1H\}$ NMR (CDCl_3): 152.45 (C5); 149.98 (C1), 136.44 (C3); 124.38 (C2); 121.38 (C4), 105.13 (C6), 63.12 (C7), 14.88 (C8). *CHN Anal.* Found: C, 38.63; H, 3.24; N, 6.55%, calculated from $C_{13}H_{14}N_2O_2Pd$ formula C, 38.31; H, 3.46; Cl, 6.87%. Theor. MS [M]$^+$ 406.2 found [M-1]$^+$ 405.3 m/z. IR, (KBr, cm^{-1}): 3450 (O−H), 3084 (Py−H); 2935−2798 (alkyl-H); 1560 (C=N); 1520−1455 (C=C), 680−500 (Pd−N).

Complex-4.
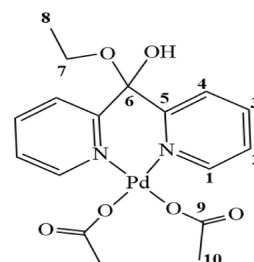
Complex-4

Yield: 68%, ^1H NMR (CDCl_3): δ (ppm): 8.92 (d, 2H, H1, J = 4.54 Hz); 8.33 (d, 2H, H4, J = 7.52 Hz); 8.23−7.90 (m, 4H, H2 and H3); 4.39 (s, 1H, OH); 3.82 (q, 2H, H7, J = 7.04 Hz); 2.23 (s, 6H, H10); 1.28 (t, 3H, H8, J = 7.02 Hz); $^{13}C\{^1H\}$ NMR (CDCl_3): 181.14 (C9); 152.45 (C5); 149.98 (C1); 136.44 (C3); 125.38 (C2); 122.38 (C4); 105.78 (C6); 62.45 (C7); 22.23 (C10); 15.08 (C8).

CHN Anal. Found: C, 44.65; H, 4.22; N, 6.35%, calculated from $C_{13}H_{14}N_2O_2Pd$ formula C, 44.90; H, 4.43; N, 6.16%, Theor. MS [M]$^+$ 455.6 found [M-1]$^+$ 454.7 m/z. IR, (KBr, cm^{-1}): 3452 (O−H), 3092 (Py−H); 2940−2800 (alkyl-H); 1635 (C=O) 1565 (C=N); 1515−1460 (C=C), 680−500 (Pd−N).

Table 1. Crystal Data and Structure Refinement of Complex-3

empirical formula	$C_{13}H_{14}Cl_2N_2O_2Pd$	
formula weight	407.56	
temperature	100(2) K	
wavelength	0.71073 Å	
crystal system	monoclinic	
space group	$P2_1/c$	
unit cell dimensions	$a = 9.7686(13)$ Å	$\alpha = 90°$
	$b = 11.9097(15)$ Å	$\beta = 93.342(2)°$
	$c = 12.5960(16)$ Å	$\gamma = 90°$
volume	1462.9(3) Å^3	
Z	4	
density (calculated)	1.850 Mg/m^3	
absorption coefficient	1.635 mm^{-1}	
$F(000)$	808	
crystal size	$0.26 \times 0.25 \times 0.14$ mm^3	
theta range for data collection	2.36 to 27.63°	
index ranges	$-12 \leq h \leq 12, 0 \leq k \leq 15, 0 \leq l \leq 16$	
reflections collected	21840	
independent reflections	3370 [$R(int) = 0.0478$]	
completeness to theta = 27.63°	98.8%	
absorption correction	semiempirical from equivalents	
max. and min. transmission	0.7673 and 0.5461	
refinement method	Full-matrix least-squares on F^2	
twin law	179.9 degrees about real axis 1, 0, 1	
twin domains ratio	0.650(1)/0.350(1)	
data/restraints/parameters	3370/0/184	
goodness-of-fit on F^2	1.107	
final R indices [$I > 2\sigma(I)$]	$R_1 = 0.0299, wR_2 = 0.0731$	
R indices (all data)	$R_1 = 0.0394, wR_2 = 0.0770$	
largest diff. peak and hole	0.769 and -0.616 e Å^{-3}	

Scheme 1. Synthesis of the Complexes
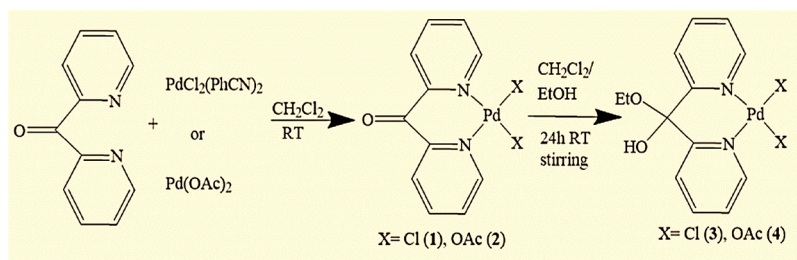
2.4. Heck Reaction. A 1.0 μmol amount of Pd(II) salt, 1.0 mmol of iodobenzene, 1.16 mol of methyl acrylate, 1.1 mmol of base, and 10 mL of DMF were combined in a 100 mL Schlenk tube. The reaction mixture underwent a freeze–thaw cycle before being heated at 80 °C for 4 h. Throughout the coupling process, samples were extracted from the reaction mixture using a dedicated syringe to monitor the extent of the conversion. After the reaction was completed, the liquid was chilled and subjected to extraction using a mixture of ethyl acetate and hexane in a ratio of 1:5. The resulting mixture was then passed through a silica gel pad with thorough washing, concentrated, and finally purified using flash chromatography on silica gel. The progress of all processes was observed by using gas chromatography (GC). The chemicals' purity was verified using NMR.

2.5. HSA and Crystallography. The HSA computational analysis was carried out via Crystal Explorer 3.1.[23] The X-ray structure determination of complex-3 was conducted by using a Bruker SMART diffractometer with graphite monochromate

Mo Kα radiation ($\lambda = 0.71069$ Å). The $P2_1/c$ space group structure was determined using a direct technique and enhanced using the SHELXL-97 computer package using full matrix least-squares analysis. The SAINT program was used to accomplish data reduction and cell refining. The calculations were conducted by using the algorithms included in the SHELXL−97 software package.[24] Table 1 contains the parameters related to the unit cell dimensions, intensity data collecting, and refinement for the structure of the compound

3. RESULT AND DISCUSSION

3.1. Synthesis, EDX, FAB-MS, and NMR. Complex-1 and complex-2 were prepared in good yields by interacting the dpk ligand with Pd(II) ions in 1:1 molar dichloromethane at RT. By adding EtOH to the reaction complex-1 or complex-2 under vigorous stirring for 24 h, the ethanoate conjugation complex-3 and complex-4 were prepared (Scheme 1). Complex-1 and complex-3 were isolated as red solids, while complex-2 and complex-4 are light oranges. All are stable in a
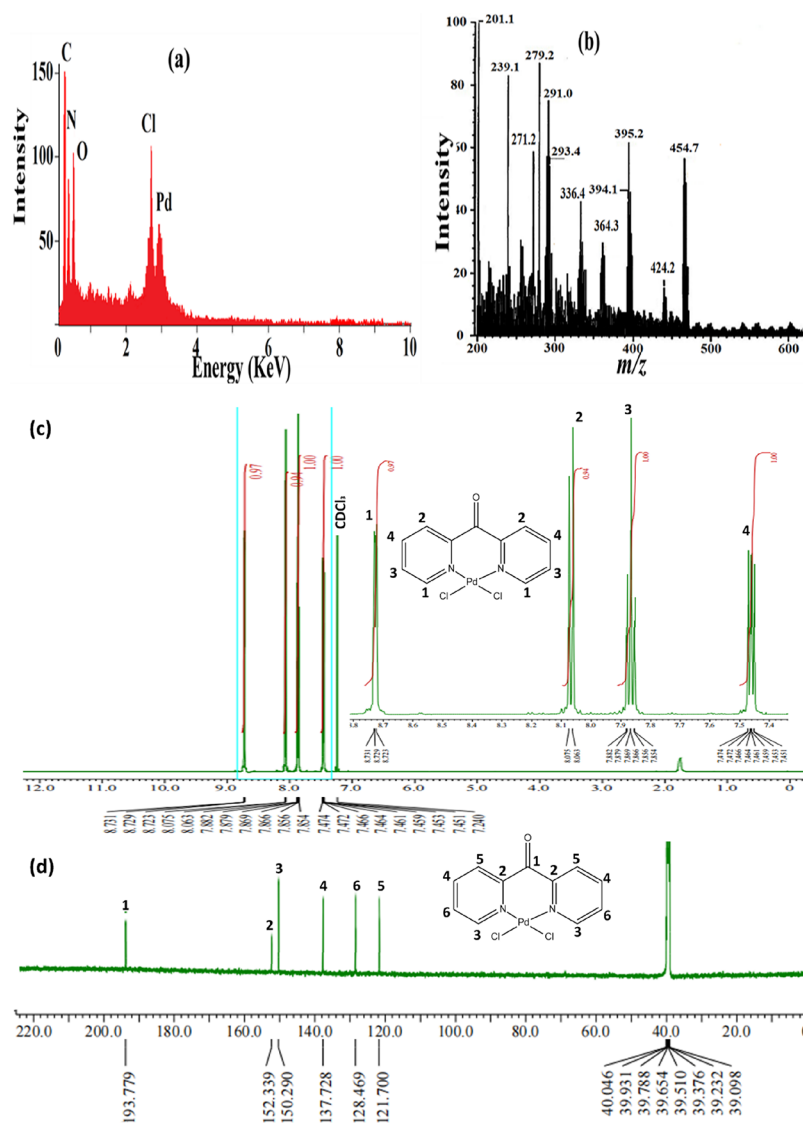
Figure 1. (a) EDX of complex-3, (b) FAB-MS, (c) ^1H NMR, and (d) ^{13}C NMR of complex-1.

solid state at RT and unstable in an open atmosphere liquid system, soluble in CH_2Cl_2, $CHCl_3$ EtOH, and MeOH, and insoluble in nonpolar solvents such as ethers or *n*-hexane.

Isolated complexes have been verified by identifying distinctive bands in IR spectra, UV–vis, CHN-EA, FAB-MS, EDX, (^1H and ^{13}C)-NMR, and XRD crystallography. The elemental analyses of these complexes are proportional to the predicted formula, as indicated in the experimental section. For example, the atomic composition of complex-3 was recorded by EDX. Figure 1a shows the energy signals consistent with the chemical content of complex-3; it displays the presence of a signal for Pd, Cl, O, N, and C only; no other signals appeared, which reflected the high degree of purity and confirmed the absence of any side products or elements contamination. In FAB-MS, peaks consistent with molecular ions of all complexes at 359.8, 408.9, 405.3, and 454.7, respectively, have been recorded. As an example, FAB-MS of complex-4 was illustrated in Figure 1b. Several m/z signals have been recorded, the peak position at 454.7 $[M]^+$ corresponding to its $C_{17}H_{20}N_2O_6Pd$ formula, together with a series of fragments 442.4 $[M-CH_3]^+$, 395.2 $[M-OAc]^+$, 364.3 $[M-OAc-OCH_3]^+$, 336.4 $[M-2OAc]^+$,

and other peaks corresponding to various undetectable fragments.

The ^1H and $^{13}C\{^1H\}$ NMR of all complexes revealed characteristic couples of signs attributed to the aromatic and allylic carbons, and protons of dpk or dpk·EtOH chelate ligands as well as the OAc group can be seen in the experimental section. For example, ^1H and $^{13}C\{^1H\}$ NMR of complexes-1–4 are illustrated in Figure 1c,d, and Figures S1, S2, and S3, respectively.

3.2. IR and UV–vis Investigations. The synthetic reactions of all complexes were tracked by FT-IR, as shown in Figure 2a and Figure S4. The substitution of both PhCN ligands from the $PdCl_2(PhCN)_2$ starting complex by dpk was proven via the demised characteristic PhCN band at 2260 cm^{-1} conforming $(dpk)PdCl_2$ production (i.e., complex-1), as shown in Figure 2a. Moreover, the disappearance of dpk O = C at 1655 cm^{-1} in complex-1 parallel to the appearances of OH at 3340 cm^{-1} and C_{alkyl}-H at 2870 cm^{-1} due to the EtOH nucleophilic in situ addition reaction resulting in $PdCl_2(dpk.EtOH)$ complex-3 was recorded as in Figure 2a. In general, FT-IR spectra of all complexes reflected character-istic peaks at 3340 cm^{-1} attributed to $v(O-H)$ in complex-3
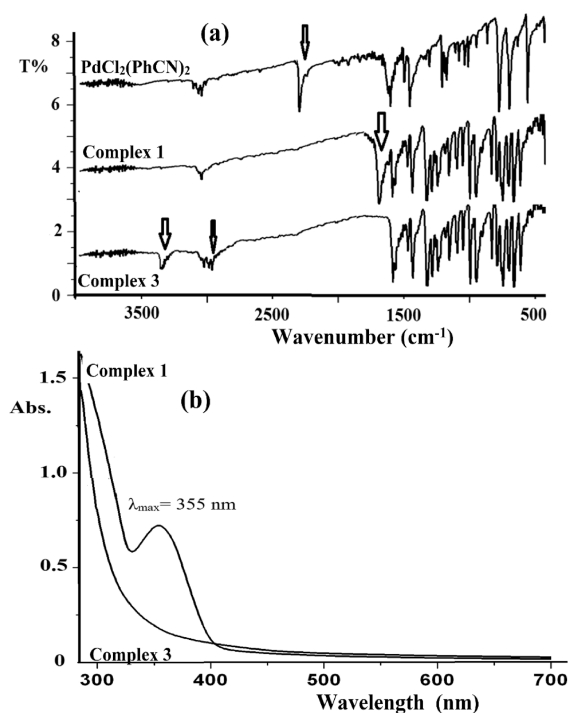
Figure 2. (a) FT-IR spectra of PdCl$_2$(PhCN)$_2$, complex-1, and complex-3; (b) electronic UV−vis spectra of complex-1 and complex-3 in EtOH at RT.

and complex-4, 3100−3050 cm^{-1} cited to $v(C_{Py}$−H), 2950−2850 cm^{-1} assigned to $v(C_{alkyl}$−H) in complex-2, 3, and 4, the C = O of dpk ligand (complex-1 and 2) and OAc bands in (complex-2 and 4) appeared at broad bands 1600−1660 cm^{-1},

and bands at 620−500 cm^{-1} attributed to $v(Pd$−N) in all complexes.[20−22]

The effect of the EtOH nucleophilic addition reaction in PdCl$_2$(dpk) to produce PdCl$_2$(dpk.EtOH) was monitored by studying the optical properties of the complexes. Figure 2b displays the UV−vis spectra of complex-1 and complex-3; both complexes showed several bands assigned to the π to π* electron transition of the dpk and (dpk·EtOH) ligand coordinated to the Pd(II) center similar to the free ligands. The band at 355 nm belongs to PdCl$_2$(dpk) in the complex-1, and the disappearance of this band upon the EtOH addition to preparing complex-3 confirmed the nucleophilic addition at the C=O of dpk, since e-delocalization was cut by such addition as seen in Figure 2b. Similar optical behaviors were observed for complex-2 and complex-4 (Figure S5).

3.3. Crystallography of PdCl$_2$(dpk·EtOH)$_3$. Complex-3 was crystallized in a CH$_2$Cl$_2$ solution with a monomeric system and square planar geometry. A light red block crystals were yielded, and a suitable specimen was chosen for XRD examination. Figure 3a shows the 3D structure of complex-3.

All the structure parameters, including angles and bond distance, are illustrated in Table 2. In situ, nucleophilic EtOH addition to the C=O of dpk in complex-1 resulted in PdCl$_2$(dpk·EtOH) complex-3. XRD analysis confirms the molecular structure of complex-3, conclusive evidence for this reaction. The previous reports indicated the hydrolysis or alcoholism of free dpk followed by coordination to the Pd(II) center.[25−28] Moreover, earlier studies have described similar structures involving PdC$_{l2}$ using the dpk·H$_2$O.[3] The two nitrogen atoms of the dpk·EtOH ligand and two chlorine atoms coordinated to the palladium center are a *cis* configuration, forming a regular square planar structure as required via the bidentate chelating geometry of the dpk·EtOH
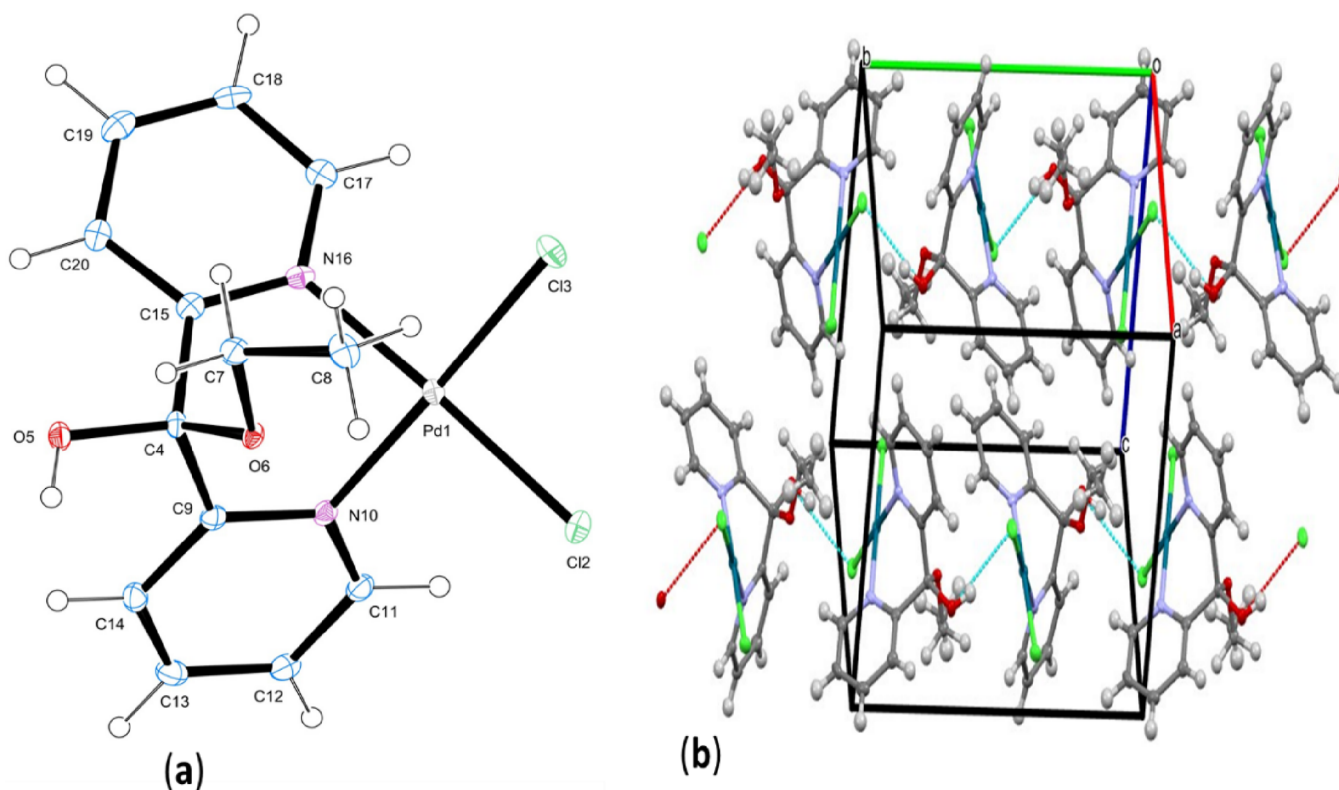
Figure 3. (a) ORTEP diagram and (b) 1D-interaction along with the unit cell of complex-3.

Table 2. Angles and Bond Lengths of Complex-3

no.	bond		Å	no.	angle			(deg)
1	Pd1	Cl2	2.2951(9)	1	Cl2	Pd1	Cl3	90.82(3)
2	Pd1	Cl3	2.294(1)	2	Cl2	Pd1	N10	90.73(8)
3	Pd1	N10	2.025(3)	3	Cl2	Pd1	N16	176.97(8)
4	Pd1	N16	2.052(3)	4	Cl3	Pd1	N10	178.39(8)
5	C4	O5	1.392(4)	5	Cl3	Pd1	N16	92.04(8)
6	C4	O6	1.412(4)	6	N10	Pd1	N16	86.4(1)
7	C4	C9	1.535(5)	7	O5	C4	O6	112.4(3)
8	C4	C15	1.525(5)	8	O5	C4	C9	111.5(3)
9	O6	C7	1.450(4)	9	O5	C4	C15	108.1(3)
10	C7	C8	1.508(5)	10	O6	C4	C9	105.6(3)
11	C9	N10	1.352(4)	11	O6	C4	C15	110.8(3)
12	C9	C14	1.384(5)	12	C9	C4	C15	108.3(3)
13	N10	C11	1.337(4)	13	C4	O6	C7	114.3(2)
14	C11	C12	1.378(5)	14	O6	C7	C8	106.7(3)
15	C12	C13	1.370(5)	15	C4	C9	N10	116.4(3)
16	C13	C14	1.380(5)	16	C4	C9	C14	122.2(3)
17	C15	N16	1.334(4)	17	N10	C9	C14	121.3(3)
18	C15	C20	1.383(5)	18	Pd1	N10	C9	119.0(2)
19	N16	C17	1.350(4)	19	Pd1	N10	C11	122.2(2)
20	C17	C18	1.387(5)	20	C9	N10	C11	118.8(3)
21	C18	C19	1.377(5)	21	N10	C11	C12	122.3(3)
22	C19	C20	1.394(5)	22	C11	C12	C13	119.2(3)
				23	C12	C13	C14	119.2(3)
				24	C9	C14	C13	119.2(3)
				25	C4	C15	N16	115.8(3)
				26	C4	C15	C20	122.8(3)
				27	N16	C15	C20	121.3(3)
				28	Pd1	N16	C15	119.6(2)
				29	Pd1	N16	C17	120.3(2)
				30	C15	N16	C17	120.0(3)
				31	N16	C17	C18	121.1(3)
				32	C17	C18	C19	119.4(3)
				33	C18	C19	C20	118.7(3)
				34	C15	C20	C19	119.4(3)

ligand. Notably, no coordination involving oxygen atoms (OH or OCH$_2$) was detected (Figure 3a). All of the angles and bond distances are given in Table 2. In the context of complex-3 crystal packing, it has been shown that the cis-protecting groups have a notable influence on the arrangement of the packing mode, as depicted in Figure 3b. The chain packing was displayed since four molecules in each unit cell (Z = 4) arrange themselves in elongated chains. These chains are connected via intramolecular hydrogen bonding, specifically O—H···O and C—H···Cl interactions, which significantly contribute to the stabilizing of the crystal lattice of complex-3.

3.4. XRD/HSA-Interactions. The synthesized Pd-complex molecule exhibited a molecular structure characterized by several H-bond types, such as C$_{alkyl}$-H···Cl/C$_{Py}$-H···O and O—H···O, which are nonclassical and classical interactions, respectively. The interactions led to the creation of two unique categories of new 2D synthons and one category of 1D interactions. The initial distinct 2D-S12 synthon connected by C$_{alkyl}$-H···Cl and C$_{Py}$-H···O with bond distances of 2.903 and 2.577 Å, respectively (Figure 4a). The second 2D-S7 synthon C$_{Py}$-H···Cl and C$_{Py}$-H···Cl with bond lengths of 2.948 and 2.943 Å (Figure 4b). Alternatively, one primary category of 1D connections was identified: O—H···O H-bonds with a bond length of 2.353 Å as seen in Figure 4c and Table 3. The presence of such synthons played a significant role in

increasing stability and manipulating material physical properties.[26]

The HSA analysis illustrated in Figure 5 provides vital information about the intermolecular interactions within complex-1 matrix.[27−30] The HSA analysis utilizes a color-mapped representation that spans from −0.454 (shown in blue) to 1.569 (shown in red) to identify locations prone to substantial and insignificant interactions. The d_{norm} surface (Figure 5a) exhibited six red spots, which signify the number of H-bond interactions per molecule. These interactions include a major nonclassical C$_{py}$-H···Cl interaction and a minor C$_{alkyl}$-H···Cl interaction as well as classical O—H···Cl hydrogen bond interactions. The shape index (Figure 5b) demonstrates the presence of electron concentrations surrounding functional groups, as indicated by surface colors that vary from red (Cl and O) to blue (alcohol proton and H's of py). The presence of a blue color surrounding surface atoms, especially H atom e-acceptors, along with the red color indicating Cl and O e-donors (Figure 5b), aided in the creation of polarized molecules via several H-bonds. In addition, the 2D-FP calculations, depicted in (Figure 5d), confirmed the existence of intermolecular contacts and disclosed the proportionate contribution of atom-to-atom interactions ratio as H···H(40%)>Cl···H(10%)>C···H(8%)>O···H(5%) > N···H(1%) > Pd···H(1%). Significantly, the Cl atoms make more
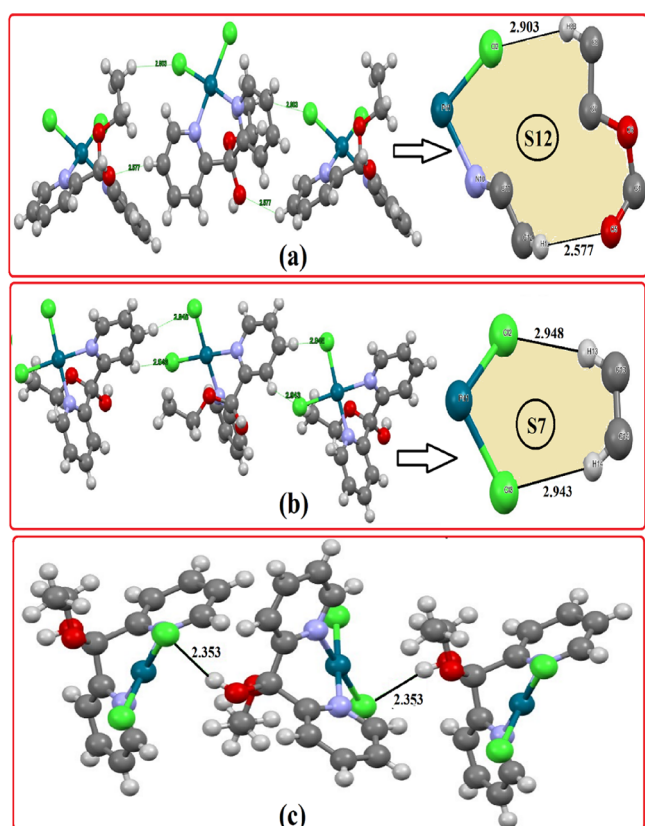
Figure 4. (a) 2D-S12, (b) 2D-S7 synthons, and (c) 1D-interactions of complex-3.

Table 3. Main Interactions Exhibited by (dpk·EtOH)PdCl$_2$

donor---H···acceptor	D-H (Å)	H···A (Å)	D···A (Å)	D-H···A (deg)
O1—H1A···Cl2	0.838	2.353	3.169	164.0
C2---H2···O1	0.951	2.577	3.299	133.0
C4—H4···O1	0.950	2.448	2.779	100.3

contributions than the O atoms, which, in turn, are greater than the contributions of N atoms. This observation is consistent with empirical XRD findings in the crystal lattice, where Cl's as e-donors are shown to be the predominant element in forming H-bonds, leading to the creation of many synthons followed by O's. However, N does not tend to engage in hydrogen bonding, which explains its 1% 2D-FP value.

3.5. TGA Investigation. The TG/DTG curves of complex-1 and complex-3 were performed in an open atmosphere temperature range of 0−1000 and 10 °C/min heating rate (Figure 6). The two complexes exhibited similar thermal behavior, and both were decomposed to PdO in one step. In complex-1, the dpk and Cl ligands were digested to light gases at 245−360 °C with a mass loss of 65.8% (calcd 66.2%) and T_{DTG} = 285 °C(Figure 6). Similarly, in complex-3, dpk·EtOH and Cl ligands were decomposed to light gases at 285−380 °C with a mass loss of 68.1% (calcd 69.2%) and T_{DTG} = 325 °C (Figure 6). Moreover, in both complexes, the PdO final decomposition product was found to be stable until ∼750 °C, above 750 to 785 °C the PdO was deoxygenated to produce pure Pd with a mass loss of ∼5.0% (calcd 5.6%) and T_{DTG} = 766 °C for complex-1 (28%, yield) and T_{DTG} = 772 °C for complex-3 (24%, yield). While the behavior of the two complexes was comparable, complex-3 exhibited greater

stability. It started to break down at a temperature 40 °C higher than complex-1, as indicated by the higher value of the T_{DTG}. This result is expected, as the alcoholization process of complex-1 introduced additional hydroxyl and ether polar functional groups to form complex-3. These extra groups contributed to enhanced bonding through hydrogen bonds, resulting in improved thermal stability of complex-3.

3.6. Heck Reaction. Heck reaction catalyzed with the prepared four complexes using methyl acrylate with iodobenzene to synthesize the cinnamate was taken as a model reaction in order to evaluate the catalytic activities of all complexes. The reactions were carried out with KOH or Et$_3$N base as cocatalysts and DMF solvent at 80 °C for ∼1 to 24 h (Scheme 2) (Table 4).

In general, traces of unwanted product were observed by GC; all complexes exhibited significant activity under basic C−C coupling conditions, and the cinnamate was obtained in a good TOF and high yield (Table 4, runs 1−7). For all catalyzed reactions, the progress of each reaction was tracked every 10 min by GC. The active reaction was detected once the conversion was almost completed in approximately 1 h (where the value TON = TOF). Under the same conditions, The catalysts improvements were recorded, exhibiting the following sequence activities: complex-3 ≥ complex-4 ≫ complex-1 ≥ complex-2 (Table 4, runs 1−4). Temperature is critical in enhancing activities; for example, using complex-3, full conversions were reached at 80 °C after 1 h; meanwhile, only 97% conversion was reached after 24 h, which reduced the TOF values (Table 4, runs 3 and 8). The base strength enhanced the coupling reaction, and the KOH, as a strong base, accelerated the process better than the weaker NEt$_3$N one (Table 4, runs 1, 3−7). Moreover, it was observed that no coupling reaction proceeded without base (Table 4, run 9); such a result is consistent with current ones.[16−21] Regrettably, all catalysts are sensitive to O$_2$, so coupling should be performed in an inert environment to prevent catalyst poisoning. Experimental results have shown that the coupling reaction never happens before getting rid of dissolved O$_2$ in solvent via Ar-degassed (Table 4, run 10). In a single experiment, when the conversion reached 50%, atmospheric O$_2$ was allowed to enter into the Schlenk tube of the reaction. However, no additional yield was seen after the reprocess reaction, even for 48 h. This indicated that atmospheric oxygen molecules can easily deactivate or poison the catalyst.

3.7. 1BNA Docking. In-silico docking is the best theoretical bioinformatic technique used here to discover and differentiate the DNA-binding tendency and nature of interactions between complex-1 and complex-3 (before and after EtOH nucleophilic addition), as seen in Figure 7. The favorable binding sites are controlled by the molecular volume as well as surface functional groups[31−34]; since complex-1 is smaller in volume, it impeded effectively in a middle minor groove position (Figure 7a), while complex-3 is a terminal side of 1BNA as seen in Figure 7b. The binding of complex-3 to the active sites of DNA is strengthened mainly by two short H-bonds as DNA:A:DA5:H3:O with 2.012 Å distance and DNA:A:DG4:O with 1.944 Å distance (Figure 7d); meanwhile, complex-1 reflected only one H-bond of type DNA:B:DA18:H3:O=C with 1.704 Å short distance (Figure 7c), it is noticed that EtOH nucleophilic addition polarized complex-3 with $^-$OH and OR functional groups which played the main role in forming H-bond interactions with the DNA. In contrast, complex-1 has more van der Waals forces
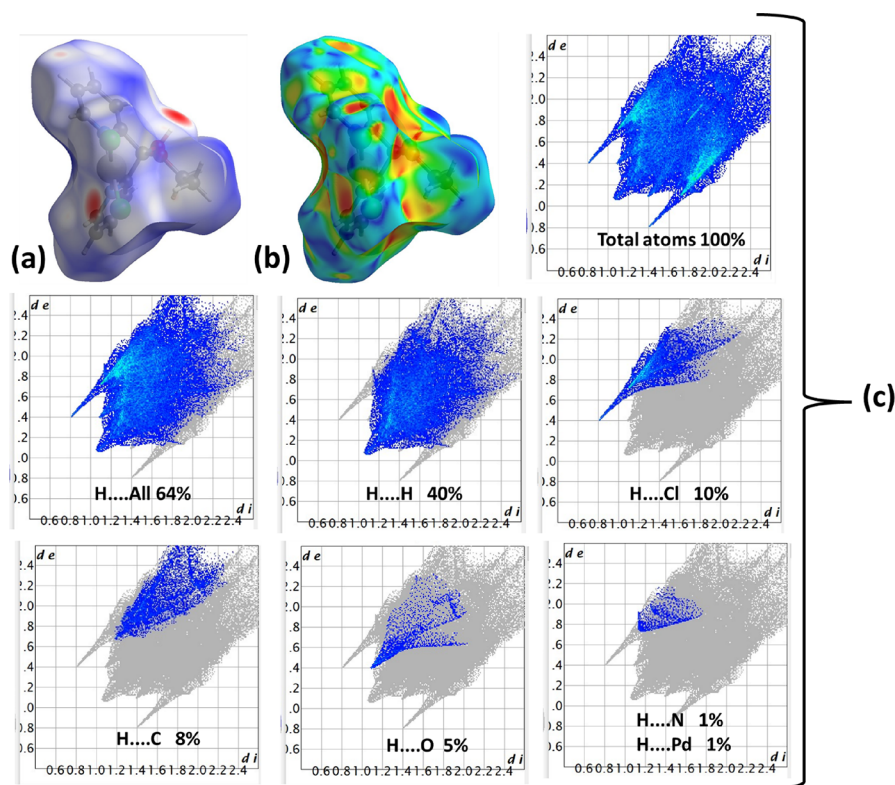
Figure 5. 3D HSA mapped over (a) d_{norm}, (b) shape index, and (c) 2D-FP plot view of the atomic contribution ratio for complex-1.
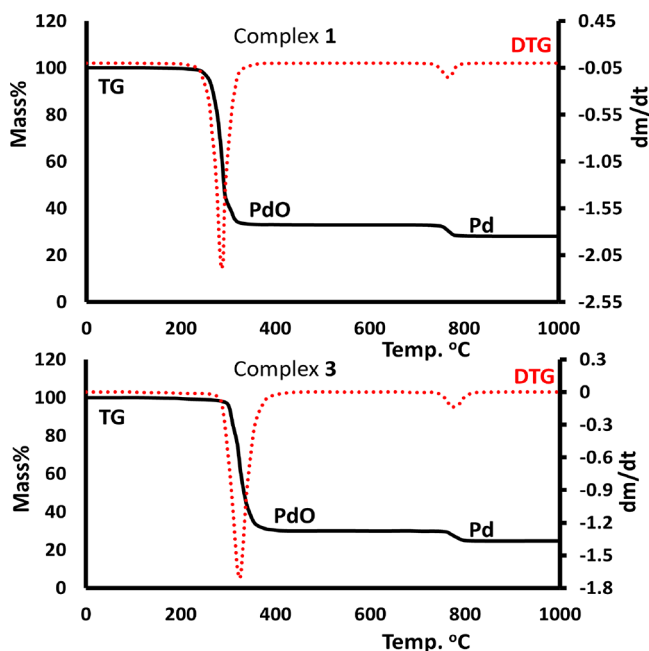
Figure 6. TG/DTG thermal behavior of complex-1 and complex-3.

Scheme 2. C−C Coupling Reaction Using the Four Complexes as Catalysts

interacting with six nuclides like DCA:9, DGA:10, DTB:19, DTB:20, DTA:8, and DAB:17(Figure 7e); meanwhile,

Table 4. Heck Couplings Catalyzed by the Four Complexes[a]

run	cat.	base	t (h)	cov. (%)	TOF
1	complex-1	KOH	2.3	99	425
2	complex-2	KOH	2.5	95	380
3	complex-3	KOH	1	99	990
4	complex-4	KOH	1	97	970
5	complex-3	Et$_3$N	1	92	920
6	complex-4	Et$_3$N	1	88	880
7	complex-1	Et$_3$N	2	75	375
8	complex-3	KOH	24	97[b]	40
9	complex-3	-	24	0[c]	0
10	complex-3	KOH	24	0[d]	0

[a]Reaction conditions: Pd(II) = 1.0 μmol, iodobenzene = 1 mmol, methyl acrylate = 1.1 mmol, base = 1.1 mmol, in 10 mL DMF at 80 °C, isolated yields are based on iodobenzene, TON = 1000, all reactions were monitored by GC. [b]RT. [c]No base was added. [d]Reaction in an O$_2$ open atmosphere.

complex-3 interacted with four nuclides DCB:23, DAA:6, DCA:3, and SER DGA:2(Figure 7h), which is not surprising since complex-1 is less polar than complex-3. The negative value of the binding energy signified complex-3 with the lowest energy (−6.92 kcal/mol) compared to complex-1 with −5.62 kcal/mol to be a better and more effective DNA binder than nonalcoholate complex-1. Nevertheless, both complexes are good binders but are one-helix DNA interactions, resulting in an anticisplatin complexes model.

4. CONCLUSIONS

In a very good yield and via an in situ nucleophilic EtOH addition reaction, four Pd(II) complexes [(dpk)PdX$_2$] and [(dpk·EtOH)PdX$_2$] (X = Cl, OAc) have been prepared. The
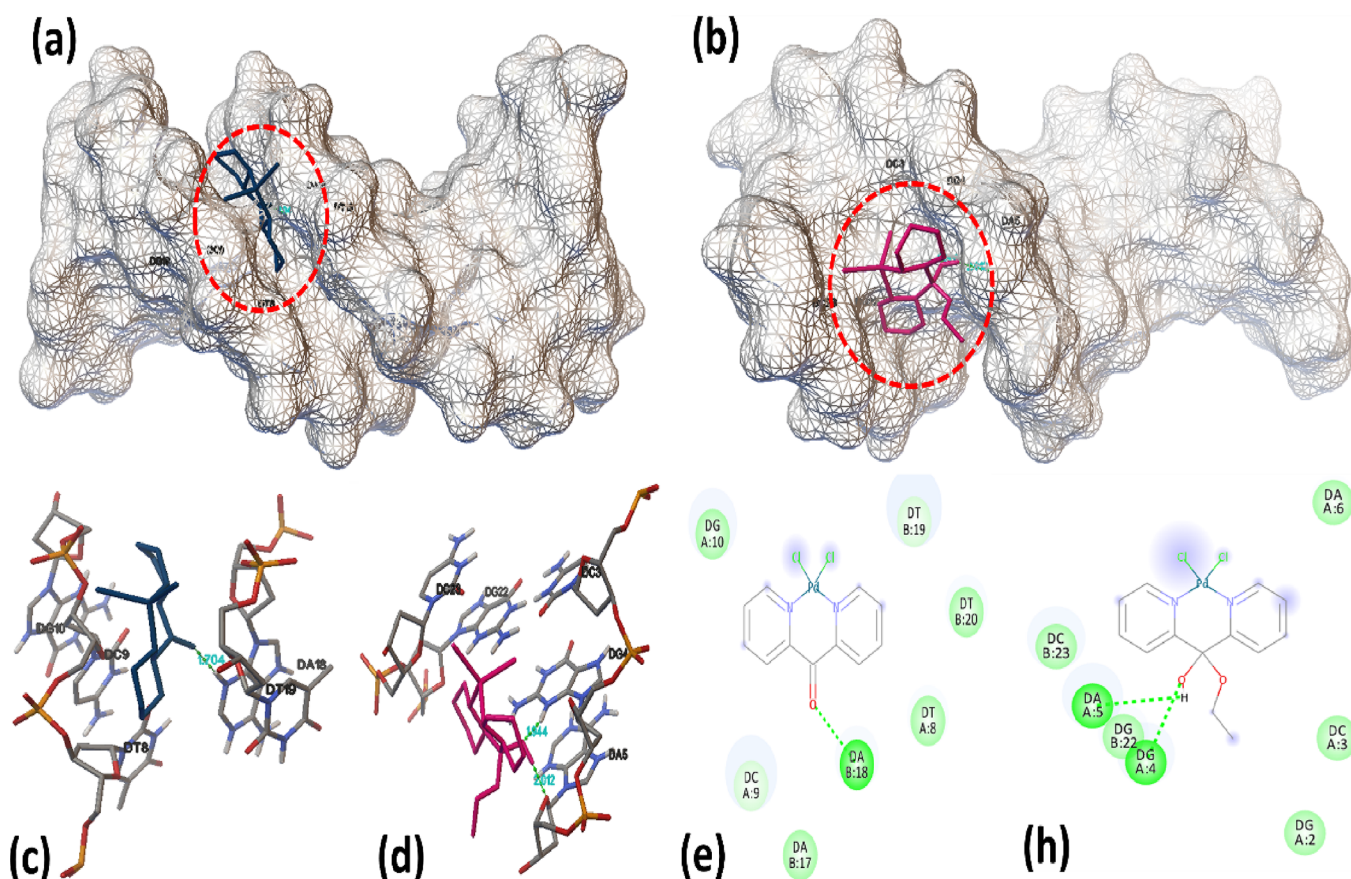
Figure 7. Docking result of complex-1 and complex-3: (a, b) minor groove interactions, (c, d) H-bond interactions, and (e, h) 2D-interactions including van der Waals forces, respectively.

EtOH addition reaction to (dpk)PdCl$_2$ resulting in (dpk·EtOH)PdCl$_2$ has been tracked by FT-IR and UV−vis. Moreover, the final structure of (dpk·EtOH)PdCl$_2$ was proven by XRD in addition to FAB-MS, EDX, CHN-EA, and NMR analyses. The XRD showed the 3D-structure complex with a square planar Pd(II) center, two types of 2D-synthons, and one 1D-interaction constructed via C$_{alkyl}$-H···Cl/C$_{py}$-H···Cl and C−O−H···O H-bonds have been proven in the crystal lattice of the complex-3. Additionally, the HSA computational analysis confirmed the existence of such classical and nonclassical H-bonds. TGA reflected complex-1 and complex-3 with similar thermal behaviors, but complex-3 had more significant stability. All four complexes reflected under mild conditions are efficient catalysts in the complex-3 ≥ complex-4 ≫ complex-1 ≥ complex-2 sequence order when methyl acrylate with iodobenzene is used as a model reaction coupled via the Heck reaction. The in silico docking result reflected the (dpk·EtOH)PdCl$_2$ as a better DNA binder than the non-alcoholate (dpk)PdCl$_2$ one.

ASSOCIATED CONTENT

Supporting Information

The Supporting Information is available free of charge at https://pubs.acs.org/doi/10.1021/acsomega.4c02015.

UV−vis, FT-IR, ^{1}H NMR, and ^{13}C NMR spectra of complex-2 and complex-4 (PDF)

AUTHOR INFORMATION

Corresponding Authors

Ismail Warad — *Department of Chemistry, AN-Najah National University, Nablus 00970, Palestine;* orcid.org/0000-0001-8853-8961; Email: warad@najah.edu

Shaukath Ara Khanum — *Department of Chemistry, Yuvaraja's College, University of Mysore, Mysuru, Karnataka 570 006, India;* orcid.org/0009-0004-8248-9053; Email: shaukathara@yahoo.co.in

Authors

Anas AlAli — *Department of Chemistry, Yuvaraja's College, University of Mysore, Mysuru, Karnataka 570 006, India*

Khalil Shalalin — *Department of Dentistry and Dental Surgery, Faculty of Medicine and Health Sciences, An-Najah National University, Nablus 00972, Palestine*

Abeer AlObaid — *Department of Chemistry, College of Science, King Saud University, Riyadh 11451, Saudi Arabia*

Khaled Alkanad — *Department of Studies in Physics, University of Mysore, Mysuru 570 006, India;* orcid.org/0000-0001-7746-3108

Abdelkader Zarrouk — *Laboratory of Materials, Nanotechnology, and Environment, Faculty of Sciences, Mohammed V University in Rabat, Agdal-Rabat 10500, Morocco; Research Centre, Manchester Salt & Catalysis, Manchester M15 4AN, United Kingdom;* orcid.org/0000-0002-5495-2125

Complete contact information is available at:
https://pubs.acs.org/10.1021/acsomega.4c02015

Notes

The authors declare no competing financial interest.

The crystallographic data has been submitted to the Cambridge Crystallographic Data Centre and assigned the additional publication number CCDC 866148. To receive copies of this information, you can visit the Web site www.ccdc.cam.ac.uk/conts/retrieving.html. Alternatively, you can contact the CCDC at their physical address: 12 Union Road, Cambridge CB2 1EZ, UK. You can also send a fax to +44−1223−336033 or an email to deposit@ccdc.cam.ac.uk. There is no charge for obtaining these copies.

■ REFERENCES

(1) Constable, E. C. *Metals and Ligand Reactivity*; VCH: Weinheim, 1996; p 261.

(2) Tasiopoulos, A. J.; Perlepes, S. P. Diol-type ligands as central 'players' in the chemistry of high-spin molecules and single-molecule magnets. *Dalton Trans.* 2008, 41, 5537.

(3) Khutia, A.; Miguel, P. J. S.; Lippert, B. Influence of PtII and PdII coordination on the equilibrium of 2, 2′-dipyridylketone (dpk) with its hydrated gem-diol form (dpk· H$_2$O). *Inorg. Chim. Acta* 2010, 363, 3048.

(4) Stamatatos, T. C.; Efthymiou, C. G.; Stoumpos, C. C.; Perlepes, S. P. Adventures in the Coordination Chemistry of Di-2-pyridyl Ketone and Related Ligands: From High-Spin Molecules and Single-Molecule Magnets to Coordination Polymers, and from Structural Aesthetics to an Exciting New Reactivity Chemistry of Coordinated Ligands. *Eur. J. Inorg. Chem.* 2009, 23, 3351.

(5) Sumby, C. J. Bridging ligands comprising two or more di-2-pyridylmethyl or amine arms: Alternatives to 2, 2′-bipyridyl-containing bridging ligands. *Coord. Chem. Rev.* 2011, 255, 1937.

(6) Tangoulis, V.; Raptopoulou, C. P.; Terzis, A.; Paschalidou, S.; Perlepes, S. P.; Bakalbassis, E. G. Octanuclearity in Copper (II) Chemistry: Preparation, Characterization, and Magnetochemistry of Cu8 (dpk⊙ OH) 8 (O2CCH3) 4 4 9H2O (dpk⊙ H2O= the Hydrated, gem-Diol Form of Di-2-pyridyl Ketone). *Inorg. Chem.* 1997, 36, 3996.

(7) Tangoulis, V.; Raptopoulou, C. P.; Paschalidou, S.; Tsohos, A. E.; Bakalbassis, E. G.; Terzis, A.; Perlepes, S. P. The Case of a Cu4 Rhombus in Molecular Magnetism: Preparation, Crystal Structure, and Magnetic Properties of Cu4(dpkCH3O)4(CH3O) 22 (dpkCH3OH= Monomethylated Diol of Di-2-pyridyl Ketone), an Example of a Cluster Allowing the Determination of All Its Exchange Parameters, Ranging from Very Strong to Very Weak. *Inorg. Chem.* 1997, 36, 5270.

(8) Aakeroy, C. B.; Champness, N. R.; Janiak, C. Recent advances in crystal engineering. *CrystEngComm* 2010, 12, 22.

(9) Szpakolski, K. B.; Latham, K.; Rix, C. J.; White, J. M. Di(2-pyridyl) Ketone Complexes of CuI- and CuII-Containing Iodide and Thiocyanate Ligands: An Unusual Case of a Mixed-Aldol Condensation. *Eur. J. Inorg. Chem.* 2010, 36, 5660.

(10) Fakhry, H.; El Faydy, M.; Benhiba, F.; Laabaissi, T.; Bouassiria, M.; Allali, M.; Lakhrissi, B.; Oudda, H.; Guenbour, A.; Warad, I.; Zarrouk, A. A Newly Synthesized Quinoline Derivative as Corrosion Inhibitor for Mild Steel in Molar Acid Medium: Characterization (SEM/EDS), Experimental and Theoretical Approach. *Colloids Surf. A: Physicochem. Eng. Asp.* 2021, 610, No. 125746.

(11) Heck, R. F. *Palladium Reagents in Organic Synthesis*; Academic Press: London, 1985.

(12) Demeijere, A.; Meyer, F. E. Fine feathers make fine birds: The Heck reaction in modern garb. *Angew. Chem., Int. Ed. Engl.* 1995, 33, 2379.

(13) JEFFERY, T. Recent Improvements and Developments in Heck-Type Reactions and Their Potential in Organic Synthesis. *Adv. Met-Org. Chem.* 1996, 5, 153.

(14) Herrmann, W. A.; Boehm, V. P. W.; Reisinger, C. P. Application of palladacycles in (15) Heck type reactions. *J. Organomet. Chem.* 1999, 576, 23.

(15) Yu, X. J.; Zhou, R.; Zhang, Y.; Fu, H. Y.; Li, R. X.; Chen, H.; Li, X. J. Heck coupling reaction catalyzed by [(C3H5) PdCl] 2-N, N, N′, N′-tetra(diphenylphosphinomethyl)-1,2-ethylenediamine. *Catal. Comm.* 2010, 12, 222−227.

(16) Trzeciak, A. M.; Ziolkowski, J. J. Structural and mechanistic studies of Pd-catalyzed CC bond formation: The case of carbonylation and Heck reaction. *Coord. Chem. Rev.* 2005, 249, 2308−2331.

(17) Aydemir, M.; Durap, F.; Baysal, A.; Akba, O.; Gümgüm, B.; Özkar, S.; Yıldırım, L. T. Synthesis and characterization of new bis(diphenylphosphino)aniline ligands and their complexes: X-ray crystal structure of palladium(II) and platinum(II) complexes, and application of palladium(II) complexes as pre-catalysts in Heck and Suzuki cross-coupling reactions. *Polyhedron* 2009, 28, 2313−2323.

(18) Shiotsuka, M.; Tanamachi, T.; Urakawa, T.; Matsuda, Y. Synthesis and structure of platinum(II)− and palladium(II)−phosphorin complexes in solid and solution state. *J. Mol. Struct.* 2006, 794, 215−220.

(19) Alonso, F.; Beletskaya, I. P.; Yus, M. Non-conventional methodologies for transition-metal catalysed carbon−carbon coupling: a critical overview. Part 1: The Heck reaction. *Tetrahedron* 2005, 61, 11771−11835.

(20) Chiusoli, G. P.; Catellani, M.; Costa, M.; Motti, E.; Della Ca', N.; Maestri, G. Catalytic C−C coupling through C−H arylation of arenes or heteroarenes. *Coord. Chem. Rev.* 2010, 254, 456−468.

(21) Warad, I.; Azam, M.; Karama, U.; Al-Resayes, S.; Aouissi, A.; Hammouti, B. Synthesis, spectroscopic characterization and catalytic significance of Palladium (II) complexes derived from 1,1 bis-(diphenylphosphinomethyl)ethane. *J. Mol. Struct.* 2011, 1002, 107−113.

(22) Azam, M.; Hussain, Z.; Warad, I.; Al-Resayes, S. I.; Khan, M. S.; Shakir, M.; Trzesowska-Kruszynska, A.; Kruszynski, R. Novel Pd(II)-salen complexes showing high in vitro anti-proliferative effects against human hepatoma cancer by modulating specific regulatory genes. *Dalton Trans.* 2012, 41 (35), 10854.

(23) Nasaruddin, N. H.; Ahmad, S. N.; Sirat, S. S.; Tan, K. W.; Zakaria, N. A.; Mohamad Nazam, S. S.; Rahman, N. M. M. A.; Mohd Yusof, N. S.; Bahron, H. Synthesis, Structural Characterization, Hirshfeld Surface Analysis, and Antibacterial Study of Pd(II) and Ni(II) Schiff Base Complexes Derived from Aliphatic Diamine. *ACS Omega* 2022, 7, 42809−42823.

(24) Sheldrick, G. M. *SHELXS-97*; University of Göttingen: Göttingen, Germany, 1997.

(25) Andrade-López, N.; Alvarado-Rodríguez, J. G.; González-Montiel, S.; Rodríguez-Méndez, M. G.; Páez-Hernández, M. E.; Galán-Vidal, C. A. cis-Palladium(II) complexes of derivatives of di-(2-pyridyl)methane: Study of the influence of the bridge group in the coordination mode. *Polyhedron* 2007, 26, 4825−4834.

(26) Bru, F.; Lesieur, M.; Poater, A.; Slawin, A. M. Z.; Cavallo, L.; Cazin, C. S. J. A Versatile Palladium Synthon: [Pd(NHC)(PhC≡CPh)]. *Chem. - Eur. J.* 2022, 28, No. e202201917.

(27) AlAli, A.; Khamees, H. A.; Madegowda, M.; Zarrouk, A.; Kumara, K.; El-khatatneh, N.; Warad, I.; Khanum, S. A. One-pot reproducible Sonosynthesis of trans-[Br(N∩N′)Cu(μBr)₂Cu(N∩N′)-Br] dimer: [H···Br S(9)] synthons, spectral, DFT/XRD/HSA, thermal, docking and novel LOX/COX enzyme inhibition. *J. Mol. Struct.* 2023, 1275, No. 134626.

(28) AlAli, A.; Al-Noaimi, M.; AlObaid, A.; Khamees, H. A.; Zarrouk, A.; Kumara, K.; Warad, I.; Khanum, S. A. Jahn-Teller distortion in SP-like [Cu(bipy)(triamine)]·2BF4 complexes with novel NH···F/CH···F synthon: XRD/HSA-interactions, physicochemical, electrochemical, DFT, docking and COX/LOX inhibition. *J. Mol. Liq.* 2023, 387, No. 122689.

(29) Bozza, G. F.; de Farias, R. L.; de Souza, R. F.; Rocha, F. V.; Barra, C. V.; Deflon, V. M.; de Almeida, E. T.; Mauro, A. E.; Netto, A. V. Palladium orthometallated complexes containing acetophenoneoxime: Synthesis, crystal structures and Hirshfeld surface analysis. *J. Mol. Struct.* **2019**, *1175*, 195−203.

(30) Saleemh, F. A.; Musameh, S.; Sawafta, A.; Brandao, P.; Tavares, C. J.; Ferdov, S.; Barakat, A.; Ali, A. A.; Al-Noaimi, M.; Warad, I. Diethylenetriamine/diamines/copper (II) complexes [Cu(dien)-(NN)]Br2: Synthesis, solvatochromism, thermal, electrochemistry, single crystal, Hirshfeld surface analysis and antibacterial activity. *Arab. J. Chem.* **2017**, *10*, 845−858.

(31) Al-Zaqri, N.; Suleiman, M.; Al-Ali, A.; Alkanad, K.; Kumara, K.; Lokanath, N. K.; Zarrouk, A.; Alsalme, A.; Alharthi, F. A.; Al-Taleb, A.; Alsyahi, A.; Warad, I. Exo⇔Endo Isomerism, MEP/DFT, XRD/HSA-Interactions of 2,5-Dimethoxybenzaldehyde: Thermal, 1BNA-Docking, Optical, and TD-DFT Studies. *Molecules* **2020**, *25*, 5970.

(32) Dhaduk, M. P.; Dabhi, R. A.; Bhatt, B. S.; Bhatt, V. D.; Patel, M. N. Palladium(II)-quinoxaline based complexes: DNA/BSA binding, DFT, docking and anticancer activity. *Mater. Today: Proc.* **2022**, *65*, 221−227.

(33) Singh, A.; Priya Gogoi, H.; Barman, P. Comparative study of Palladium(II) complexes bearing tridentate ONS and NNS Schiff base ligands: Synthesis, characterization, DFT calculation, DNA binding, bioactivities, catalytic activity, and molecular docking. *Polyhedron* **2022**, *221*, No. 115895.

(34) Onunga, D. O.; Omondi, R. O.; Sitati, M.; Mutua, G. K.; Jaganyi, D.; Mambanda, A. Biomolecular interactions of 1,3-bis(2-arylimino)isoindolate-based Palladium(II) complexes: Substitution kinetics, DNA/protein-binding, and molecular docking approaches. *Inorg. Chim. Acta* **2023**, *558*, No. 121730.